TU Delft

Delft University of Technology

# Operating characteristics of an electrically assisted turbofan engine

van Holsteijn, M.R.; Gangoli Rao, A.; Yin, F.

**DOI**
10.1115/GT2020-15355

**Publication date**
2020

**Document Version**
Final published version

**Published in**
Aircraft Engine; Fans and Blowers

**Citation (APA)**
van Holsteijn, M. R., Gangoli Rao, A., & Yin, F. (2020). Operating characteristics of an electrically assisted turbofan engine. In *Aircraft Engine; Fans and Blowers* Article GT2020-15355 (Proceedings of the ASME Turbo Expo; Vol. 1). https://doi.org/10.1115/GT2020-15355

**Important note**
To cite this publication, please use the final published version (if applicable).
Please check the document version above.

**Copyright**
Other than for strictly personal use, it is not permitted to download, forward or distribute the text or part of it, without the consent of the author(s) and/or copyright holder(s), unless the work is under an open content license such as Creative Commons.

**Takedown policy**
Please contact us and provide details if you believe this document breaches copyrights.
We will remove access to the work immediately and investigate your claim.

*This work is downloaded from Delft University of Technology.*
*For technical reasons the number of authors shown on this cover page is limited to a maximum of 10.*

*Green Open Access added to TU Delft Institutional Repository*

*'You share, we take care!' - Taverne project*

*https://www.openaccess.nl/en/you-share-we-take-care*

Otherwise as indicated in the copyright section: the publisher is the copyright holder of this work and the author uses the Dutch legislation to make this work public.

**Proceedings of the ASME Turbo Expo 2020**
**Turbomachinery Technical Conference and Exposition**
**GT2020**
**June 22-26, 2020, London, England**

**GT2020-15355**

# OPERATING CHARACTERISTICS OF AN ELECTRICALLY ASSISTED TURBOFAN ENGINE

**Merijn Rembrandt van Holsteijn**
**Arvind Gangoli Rao***
**Feijia Yin**
Department of Aerospace Engineering
Delft University of Technology
Delft, The Netherlands
Email: A.GangoliRao@tudelft.nl

## ABSTRACT

*With the growing pressure to reduce the environmental footprint of aviation, new and efficient propulsion systems must be investigated. The current research looks at the operating characteristics of a turbofan engine in a parallel hybrid-electric propulsion system. Electric motors are used to supply power in the most demanding take-off and climb phases to achieve the required thrust, which allows the turbofan to be redesigned to maximize the cruise performance (to some extent). It was found that the turbofan's cruise efficiency can be improved by 1.0% by relaxing the constraints of take-off and climb. It was found that the surge margins of compressors limit the amount of power that could be electrically supplied.*

*On a short-range mission, the hybrid-electric propulsion system showed a potential to reduce around 7% of fuel burn on an A320 class aircraft. Most of these savings are however achieved due to fully electric taxiing. The weight of the electrical propulsion system largely offsets the efficiency improvements of the gas turbine during cruise flight. A system dedicated for fully electric taxiing system could provide similar savings, at less effort and costs. Given the optimistic technology levels used in the current analysis, parallel hybrid-electric propulsion is not likely to be used in the next-generation short to medium range aircraft.*

## NOMENCLATURE

| | |
|---|---|
| BPR | Bypass ratio [-] |
| CC | Combustion chamber |
| DDTF | Direct drive turbofan |
| EM | Electric motor |
| EATF | Electrically assisted turbofan |
| GTF | Geared turbofan |
| HEP | Hybrid electric propulsion |
| HEPS | Hybrid electric propulsion system |
| HP | High pressure |
| HPC | High pressure compressor |
| HPT | High pressure turbine |
| LP | Low pressure |
| LPC | Low pressure compressor |
| LPT | Low pressure turbine |
| M | Mach number [-] |
| MTOW | Maximum take-off weight [kg] |
| OPR | Overall pressure ratio [-] |
| P | Power [kW] |
| PR | Pressure ratio [-] |
| SLS | Sea level static |
| SM | Surge margin |
| TIT | Turbine inlet temperature [K] |
| TO | Take-off |
| TOC | Top of climb |
| TSFC | Thrust specific fuel consumption [g/kNs] |
| v | Velocity [m/s] |
| W | Massflow [kg/s] |

### Greek Symbols

| | |
|---|---|
| $\eta$ | Efficiency [%] |
| $\omega$ | Rotational speed [rad/s] |
| $\Phi$ | Power split [%] |
| $\pi$ | Pressure ratio [-] |
| $\Psi$ | Power fraction [-] |

### Subscripts

| | |
|---|---|
| C | Corrected |
| poly | polytropic |

*Address all correspondence to this author

Copyright © 2020 by ASME

**Gas Turbine Stations**

| | |
|---|---|
| 0 | Ambient |
| 1 | Inlet |
| 13 | Fan exit bypass |
| 16 | Bypass duct |
| 19 | Bypass nozzle exit |
| 2 | Fan inlet |
| 21 | Fan exit core |
| 25 | Low pressure compressor exit |
| 3 | High pressure compressor exit |
| 4 | High pressure turbine inlet |
| 49 | Low pressure turbine inlet |
| 54 | Low pressure turbine exit |
| 6 | Core duct |
| 9 | Core nozzle exit |

## 1. INTRODUCTION

In the past decade, several organisations have set goals for improving the efficiency of aircraft, including the European Commission [1]. These goals have been set to reduce the negative impact of flying on the environment in terms of emissions and noise created by the aircraft. Unfortunately, there is not yet a clear roadmap to reach these goals, as was recently presented at the 2019 World Economic Forum [2]. The $CO_2$ emission from aviation is around 2.5-3% of the anthropogenic $CO_2$ and is responsible for 5% of the anthropogenic radiative forcing when including the non-$CO_2$ effects as well [2, 3]. Aviation is, therefore, one of the major influencers in climate change; and with aviation increasing at around 5% every year, the contribution of aviation to the global climate change will increase significantly.

To mitigate the environmental impact of aviation, a promising concept that is being studied intensively in recent years is hybrid-electric propulsion (HEP). Narrow-body aircraft seems to be a promising candidate for this technology [4]. On longer-range flights, the additional weight of the electric propulsion system makes it difficult to achieve any substantial fuel saving. Multiple studies have shown that HEP can reduce the fuel burn in regional flights by around 7-10% with the envisaged 2030-2035 technology in comparison to conventional propulsion system [4, 5]. With technological levels forecasted after 2030-2035, significant fuel savings by HEP are expected to be possible, even on long haul flights [6]. Reasons for interest in this new technology go further than emission savings alone. In addition to the fuel savings and the high cost of fuel, there is an economic reason to explore this technology as well. Strategic benefits are the reduced dependence on the depleting fossil fuels and the ability to taxi with reduced noise and pollutant emissions. These potential benefits could ease the current restrictions due to noise issues on the number of aircraft movements at airports.

A hybrid-electric propulsion system (HEPS) consists of a gas turbine engine combined with an electric motor (EM) and a battery pack. Several ways are possible to connect these components in a power train. The most well-known configurations are the series and parallel type, shown in Fig. 1 and Fig. 2 respectively. In a series configuration, the gas turbine generates electricity via a generator. The electricity is then used by the EM to drive a fan/propeller to produce thrust, besides power from the generator, batteries can assist in supplying power to the EM. In the parallel type, a gas turbine is assisted in driving the fan/propeller by the EM, also named as electrically assisted turbofan (EATF). Both configurations have their advantages and disadvantages, but because the parallel configuration is closer to a conventional one, it requires fewer changes and is therefore expected to be the first step towards a HEP aircraft [5, 7].

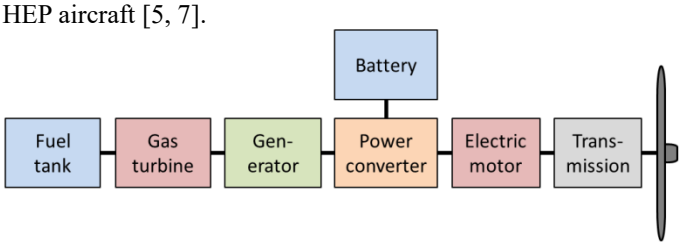


**Figure 1: Series architecture**

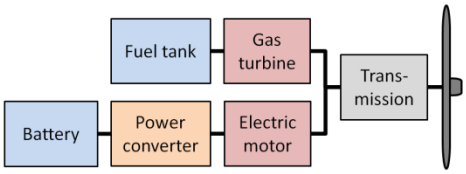


**Figure 2: Parallel architecture**

Former research on parallel EATF has considered only one EM connected to the low pressure (LP) shaft [5, 6, 7, 8]. The problem with only one EM is that it might cause the compressor to surge and could push compressors away from their most efficient operating points. A possible solution to this problem was proposed in another research [9], in which the LP and HP shaft were mechanically linked via a gearbox, thereby reducing the shift in the operating line. A downside to this solution is that an additional, heavy and complex component is placed between the power input (electrical motor) and the thrust generation. If however, the same amount of electric power would be supplied via two EMs, one on each spool, the mechanism can be simplified while allowing both spools to operate within safe surge margins and at efficient operating points. The aim of this research is therefore to find the operating characteristics and limits of an EATF with two EMs. Airbus A320neo is used as a baseline for this research as this single-aisle aircraft is a workhorse of civil aviation [10]. The reference turbofan considered in this study is the CFM LEAP-1A26, which powers the A320neo. Although the physical positioning of the EMs inside the turbofan is not analysed in this research, a possible location of EM on the HP shaft for is at the same location where the current turbofan engines have their generator for electric power (connected to the accessory gearbox). While multiple locations for connecting the EM with the LP shaft have been explored, the location inside the fan hub has been found to be promising [8].


Copyright © 2020 by ASME

The power management strategy that was suggested by [5], is used in this research. Figure 3 shows the mission power management strategy. The aircraft uses electric taxi-in and out, electrically assisted take-off and climb, and cruise on solely the gas turbine. The reasoning behind this power management strategy is that at cruise, it is best to use the gas turbine, as the specific energy density of batteries is much lower than that of kerosene. If the HEPS is used only to assist the turbofan in take-off and climb, the turbofan is no longer required to meet the thrust requirements on its own. It can then be sized specifically for cruise and thereby improve its thrust specific fuel consumption (TSFC). During taxi, the gas turbines operate at low power settings, at which they perform poorly in terms of efficiency. Electric motors do not have this problem and would, therefore, provide the thrust during taxiing. The most important operating conditions (i.e. take-off, climb and cruise) will be analysed in this research.

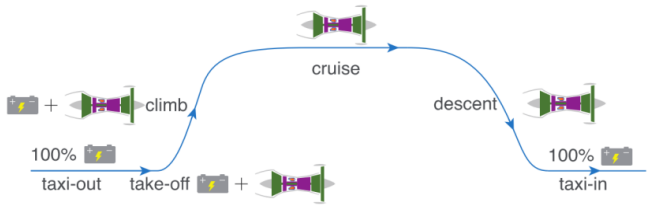


**Figure 3: Power management strategy [5]**

The intention of this study is therefore to investigate how electrical power could be supplied to the different gas turbine spools in the most power demanding phases while respecting the operating constraints and maximizing its overall efficiency. To simplify the study, the current analysis is mainly focussed on the propulsion system, while the aircraft mission, payload and airframe are assumed to remain unchanged.

## 2. MODELLING AND METHODS

Modelling of this study is divided into three aspects: gas turbine modelling, hybrid-electric propulsion system modelling and the mission profile.

### 2.1. Gas Turbine Modelling

The modular Gas Turbine Simulation Program, GSP® is used to build a gas turbine model [11]. The GSP® is a flexible component-based thermodynamic modelling environment to model various gas turbine configurations. Furthermore, GSP® can be extended with MATLAB® via the application programming interface [12]. In this way, it is also possible to model an EATF. GSP® is based on a 0-D thermodynamic model, making it very fast and suitable for performance analysis and conceptual study.

Figure 4 shows the layout of a CFM LEAP engine model that has been built in GSP®. The figure also shows the bleed control schedule (component number 1), which is used to schedule the LPC bleed-off at low LP-spool speeds to prevent surge. As is shown in the figure, the standard gas turbine components are numbered from 2 to 13. First, there is an inlet (number 2), followed by a fan (number 3) with the bypass and core exits. The fan core exit is followed by the LPC (number 4) and the HPC (number 5). Number 6 is the control for component number 7: the combustion chamber (CC). This is followed by two turbines, the HPT (number 8) and LPT (number 9). Then, aft of both the fan bypass and LPT, a duct (number 10 and 12) and an exhaust (numbers 11 and 13) are present.

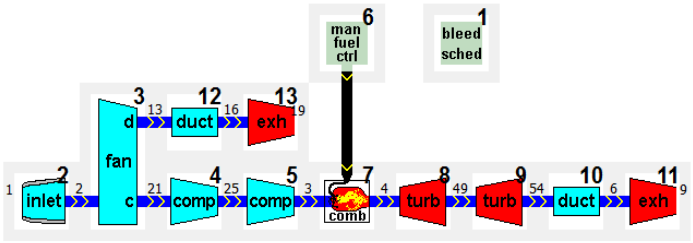


**Figure 4: CFM LEAP-1A model in GSP®**

The performance simulation follows a sequential procedure starting from a reference point (cruise condition in the current paper) and followed by off-design performance calculation at other operating conditions. The calculation at the reference point follows a standard thermodynamic procedure [13]. Generic compressor and turbine maps are used for the off-design calculations. More information on the workings of GSP® can be found in [11, 14].

#### 2.1.1. Thrust Requirements

An aircraft is required to take-off within a certain maximum distance and to climb at a specific rate. To achieve this, the gas turbine has thrust requirements at these points. At take-off, the maximum rated thrust of the selected engine is 120.6 kN at sea level static (SLS) conditions [15]. Initial cruise thrust is calculated by assuming that the amount of fuel burnt during take-off and climb is insignificant to the MTOW, so the MTOW (73.5 tonnes [16]) is divided by the cruise L/D ratio (16.8 [17]). This gives 21.5 kN of thrust per engine. To calculate the top of climb (TOC) thrust requirement, the initial cruise thrust is multiplied by a factor, as presented in another research [18]. For the same MTOW, similar aircraft require similar take-off thrust for similar performance. A320neo's predecessor, the A320ceo, was powered by the CFM56-5B4 for aircraft with similar MTOW weight and it produced the same take-off thrust as the LEAP-1A26. This CFM56 provided a TOC thrust of 25.0 kN together with an initial cruise thrust of 22.3 kN [19]. A320neo climb requirements are assumed to be the same as the A320ceo, meaning a TOC thrust requirement of 24.1 kN per engine. The average cruise thrust will be set as the reference point of the gas turbine model which is calculated by averaging the MTOW and zero fuel weight [16], and dividing the weight by the cruise L/D ratio. The average cruise thrust value calculated was 19.9 kN per engine. Table 1 summarises the thrust requirements per stage with appropriate Mach number and altitude [20].


Copyright © 2020 by ASME

**Table 1: Thrust requirements per flight segment, per engine**

| Flight segment: | Thrust: [kN] | Mach: [-] | Altitude: [m] |
|---|---|---|---|
| Take-off | 120.6 | 0.0 | 0 |
| TOC | 24.1 | 0.78 | 11280 |
| Cruise | 19.9 | 0.78 | 11280 |

### 2.1.2. Gas Turbine Validation

The TSFC is checked in several ways. First, in Table 2 the fuel consumption is compared to ICAO data [15]. At higher thrust settings the model shows good agreement (only a difference of around 2%). However, at idle, the difference in the fuel flow increases to 18.7% (7% thrust). This large deviation can be attributed to aspects such as the use of generic performance components maps instead of the actual maps, the simplification of a constant cooling flow rate at all thrust settings and the fact that the combustion efficiency is assumed constant. However, the discrepancy at idle is not expected to influence the overall results as the idle will not have a significant influence on the overall mission performance.

**Table 2: Turbofan model validation [15]**

| Thrust level: [% $F_\infty$] / [kN] | ICAO: [kg/s] | Simulation: [kg/s] | Difference: [%] |
|---|---|---|---|
| 100 / 120.6 | 0.861 | 0.879 | 2.1 |
| 85 / 102.5 | 0.710 | 0.719 | 1.3 |
| 30 / 36.2 | 0.244 | 0.248 | 1.6 |
| 7 / 8.4 | 0.091 | 0.074 | -18.7 |

The efficiency during the cruise condition is validated by combining data from multiple references. The predecessor of the LEAP-1A26, the CFM56-5B4, has a TSFC of 16.98 g/kN-s [19]. This is assumed to include power and bleed requirements for the aircraft. CFM, the manufacturer of the LEAP-engine, claims a TSFC reduction of 15% for LEAP-1A26 than CFM56-5B4 [21]. LEAP-1A26's cruise TSFC is therefore expected to be 14.43 g/kN-s. A TSFC of 14.67 g/kN-s is obtained from the current modelling, thereby implying a marginal overprediction by 1.7%. Thus, the modelled gas turbine does show overall good agreement with the actual engine.

## 2.2. Hybrid Electric Propulsion System Modelling

The EATF is modelled in the same GSP® environment. The GSP® allows power to be supplied into both the HP- and LP-spool. An important parameter in analysing HEPS is the power split (Φ), defined in Eqn. 1. It relates the total amount of electrical power supplied into the gas turbine to the total LP-shaft power. Previous research [5] showed that the power split ratio during the climb has more influence than the power split during take-off, because of the length of this phase. Around 14% climb power split was found to be optimum due to its potential fuel-saving capabilities while not exceeding the aircraft MTOW and limiting the total energy consumption. For the current analysis, a 14% power split is used for take-off as well. By having a power split of 14% in both phases, the EM can be sized for the climb in terms of power (and weight) and during take-off can be operated at peak power (about twice the amount of nominal power, as recommended in the literature [22, 23]).

$$\Phi = \frac{P_{EM\ LP-shaft} + P_{EM\ HP-shaft}}{P_{total\ LP-shaft}} \quad (1)$$

Another parameter required for modelling the EATF is the LP-power fraction (Ψ), defined in Eqn. 2 as the electrical power supplied to the LP-shaft compared to the electrical power added to both the HP and LP-shaft. An LP-power fraction of 1 implies that all electrical power is supplied to the LP-shaft and an LP-power fraction of 0 implies that all the power is supplied to the HP-shaft. The used LP-power fraction will be explained in the results section.

$$\Psi = \frac{P_{EM\ LP-shaft}}{P_{EM\ LP-shaft} + P_{EM\ HP-shaft}} \quad (2)$$

The EM is modelled by defining the five main losses inside an EM, namely: copper, iron, friction, windage and constant losses [24], along with magnetic saturation and field weakening [25]. The simulated performance maps showed good agreement with the data provided in [26]. It was found the variation in electric motor efficiency is not significant during different flight phases; therefore, for simplicity reasons average efficiency values were used in both take-off and climb phases.

The inverter and battery were simulated with a constant efficiency, power density and energy density, the values of which are shown in the section 3.3. Modelling their performance variation for different conditions are beyond the scope of this study.

## 2.3. Mission Profile

A basic short-range mission profile described in [5] is used to study the possible fuel savings. The mission comprises a 5 minutes of taxi-out, 0.7 minutes of take-off, 25 minutes of climb, 35 minutes of cruise, 20 minutes of descent and 5 minutes of taxi-in, with a mission length of 1000 km. To obtain the same mission profile for the standard A320neo and the A320 with the new HEPS, an assumption is made: the weight of the aircraft with HEPS does not influence the L/D ratio of the aircraft as the engine external dimensions are not affected significantly by the addition of the electric motor on the LP and/or HP shaft. Therefore, the thrust for the A320neo from [5] can be scaled with the weight difference between the HEP A320 and the A320neo and the mission fuel consumption is obtained by iterating.

# 3. RESULTS AND DISCUSSION

The results are divided into two parts, the first part looks at the characteristics of the EATF and the second part looks at the effect of turbofan resizing for the cruise mission.


Copyright © 2020 by ASME

### 3.1. Electrically Assisted Turbofan Characteristics

To find the characteristics of an EATF, the baseline LEAP-1A26 model is used. It is examined at SLS and TOC conditions since these are the most stringent operating conditions in terms of operational stability for the turbofan. In order to understand the sensitivity of the EATF characteristics to the amount of electric power used, three power splits (as defined in Eqn.1) are considered respectively: 14% (baseline), 7%, and 21%. The GTF architecture featuring a high-speed LPC is also compared with a DDTF to check its feasibility in an EATF configuration.

#### 3.1.1. Sea Level Static

At SLS condition, the three different power split levels, 21%, 14% and 7% correspond to 3.9 MW, 2.6 MW and 1.3 MW respectively. For a given power split ratio, the LP-power fraction (as defined in Eqn. 2) is varied from 1 to 0, to gradually increase the electric power added to the LP shaft. Accordingly, the variations in EATF operating characteristics are analysed. These results are obtained by setting GSP® to off-design calculations, with a thrust requirement of 120.6 kN for every case. GSP® finds the operating point by varying the fuel flow rate. Figure 5 shows the operating characteristics of the LPC at SLS take-off conditions. For a given power split, increasing the LP-power fraction increases the LPC pressure ratio while the corrected speed remains constant. Whereas, higher power split can increase the width of the operating line between an LP-power fraction of 1 and 0, meaning a wider operating range. It can be observed from Fig. 6 that LP-power fraction of 1 is infeasible for any power split ratio because of the violation of the LPC surge margin (SM) limit: 15% in this paper [13]. Overall, the LPC SM decreases with increasing LP-power fraction and therefore limits some combinations of power supply to the LP and the HP-spool.

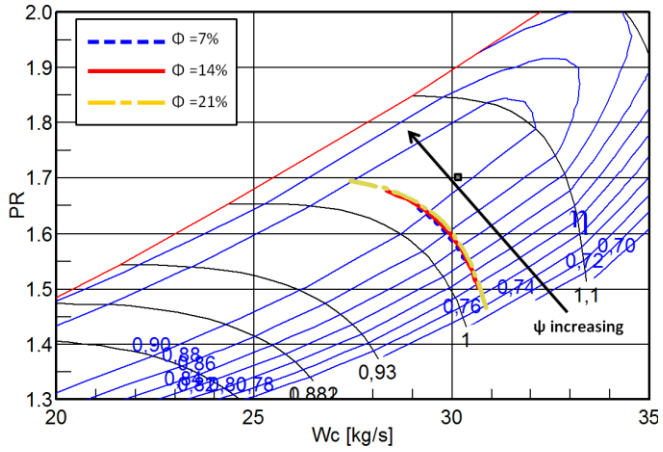


**Figure 5: Operating characteristics of the LPC at SLS TO under electrical power supply**

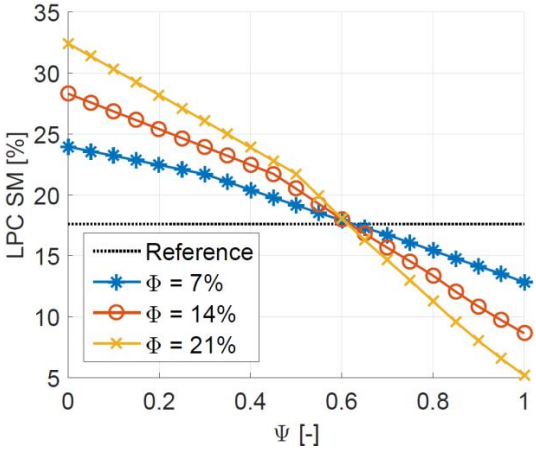


**Figure 6: LPC SM under different power splits and power fractions for DDTF**

In terms of efficiency, the goal is to minimise the thrust specific fuel consumption (TSFC) for a given combination of the electric power split and the LP-power fraction. The variation of fuel flow rate for various LP power fraction is shown in Fig. 7. As can be seen from the figure, the most efficient LP-power fraction depends on the power split that is used. It can be seen that the optimum LP-power fraction shifts to lower values for higher power split. Therefore, the larger the total power supplied to the gas turbine, the larger the fraction that needs to be supplied to the HP-spool.

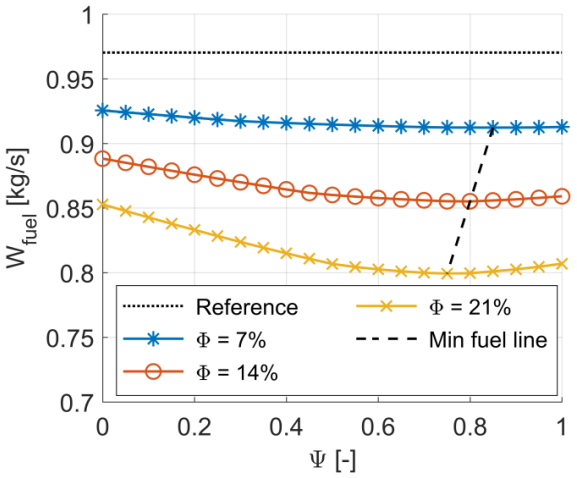


**Figure 7: Fuel flow rate under different power splits and power fractions at SLS TO conditions**

In Fig. 8, the operating points for various power splits at SLS take-off condition are shown on the HPC map. The lines show a different trend compared to those on the LPC map (Fig. 5). With increasing the LP-power fraction, the HPC pressure ratio (PR) decreases together with the corrected speed. The decrease in HPCPR is larger than the increase in LPCPR; thereby, the OPR decreases with increasing the LP-power fraction. This is the main reason why the optimum LP-power fraction is not 1. In a high BPR turbofan (such as LEAP-1A),


Copyright © 2020 by ASME

the majority of the thrust is produced by the bypass jet. For a constant thrust requirement (at a given ambient condition), the fan speed and operating conditions remain nearly unchanged. Therefore, the LP-shaft power is almost constant. With a power split of 14%, the majority of the power in the LP-shaft still needs to be provided by the LPT. Since the fuel flow rate reduces when electric power is supplied to the gas turbine, the gas power at the end of the combustion chamber reduces. This in its turn reduces HP-spool speed and the resulting HPC pressure ratio.

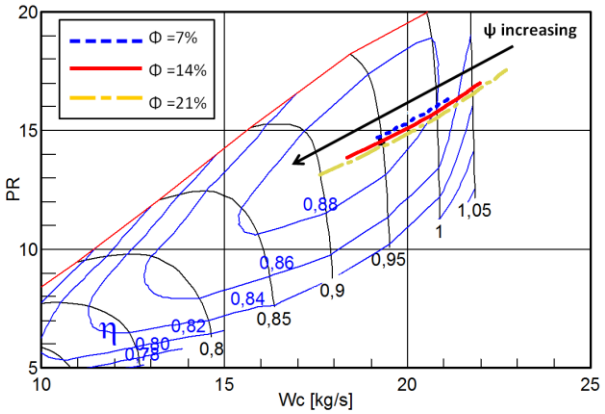


**Figure 8: Operating characteristics of the HPC at SLS Take-off for various power fractions**

### 3.1.2. Top Of Climb

At TOC, the overall trends are similar to those at SLS take-off. The same power splits (as at take-off) are used, 21%, 14% and 7%, which correspond to 2.1 MW, 1.4 MW and 0.7 MW respectively. The effective power is lower in TOC compared to SLS, because the overall power of the turbine decreases due to lower air density. At higher LPC corrected speed in TOC conditions, the SM is reduced, as shown in Fig. 9. The SM requirement limits the ability to operate at the optimum LP-power fraction. Figure 10 shows the fuel flow rate required at TOC. At 14% power split, the LP-power fraction with maximum efficiency is 0.75, but the SM is even lower than the 12% LPC SM of the baseline model. In order to operate with a safe SM, the LP-power fraction should not exceed 0.6.

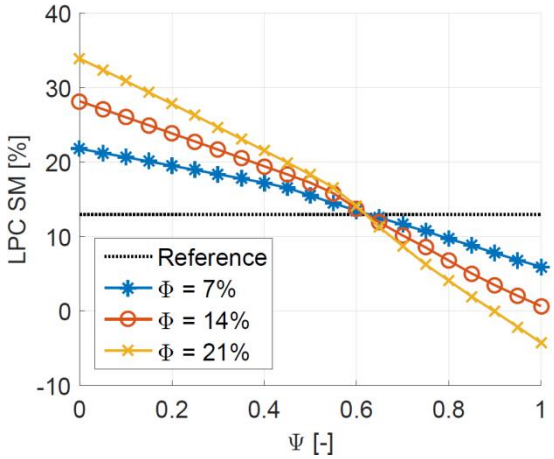


**Figure 9: LPC SM under different power splits and power fractions at TOC conditions**

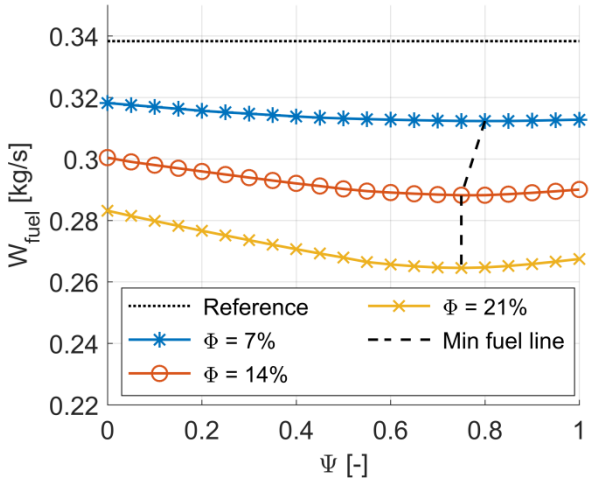


**Figure 10: Fuel flow rate under different power splits and power fractions at TOC conditions**

The feasibility of a geared turbofan (GTF) [27] for an EATF architecture is investigated by using a different LPC performance map (transonic LPC map instead of a subsonic LPC map). The results are obtained as shown in Fig. 11. The map's efficiency contours are shaped differently, and the maximum efficiency contour is positioned further away from the surge line. Figure 12 shows that the SM of the transonic LPC at TOC is clearly increased as compared to that of a direct drive turbofan (DDTF). Although the SM requirement of 15% limits the LP-power fraction to 0.7 (at 14% power split), it is close to the maximum efficiency point of 0.75. Therefore, a transonic LPC of a GTF seems to be better suited for the EATF architecture.


Copyright © 2020 by ASME

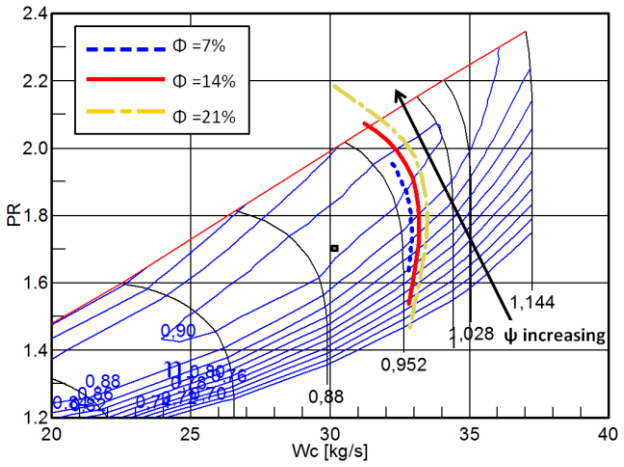


**Figure 11: Operating characteristics of the transonic GTF LPC at TOC with electrical motor assistance**

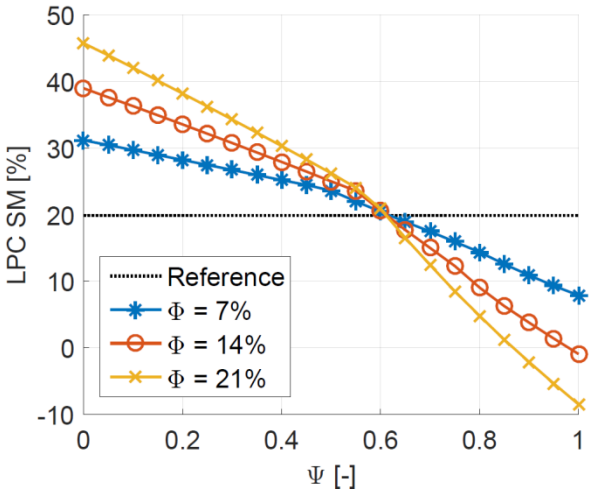


**Figure 12: Transonic LPC SM under different power splits and power fractions at TOC conditions**

### 3.2. Redesign of the Turbofan

With respect to the redesign of the turbofan for cruise conditions, Fig. 13 shows that the overall efficiency of a gas turbine can be split into thermal and propulsive efficiency. The overall efficiency is defined by Eqn. 3 [13], as the thrust power (thrust multiplied by flight speed) divided by the total supplied power to the gas turbine, which is the chemical power of the fuel together with the electrical power.

$$\eta_{total} = \frac{P_{thrust}}{P_{chemical}+P_{electrical}} \quad (3)$$

Thermal efficiency is defined by Eqn. 4 and is defined as the propulsive jet kinetic power added to the flow with respect to the total power supplied to the gas turbine. The propulsive efficiency is the conversion from propulsive jet power into thrust power (Eqn. 5). Propulsive efficiency is affected by the fan PR and the BPR of the engine. Thermal efficiency, on the other hand, depends on the efficiency of the individual components, the OPR, the pressure losses in the ducts, the combustion efficiency and the TIT.

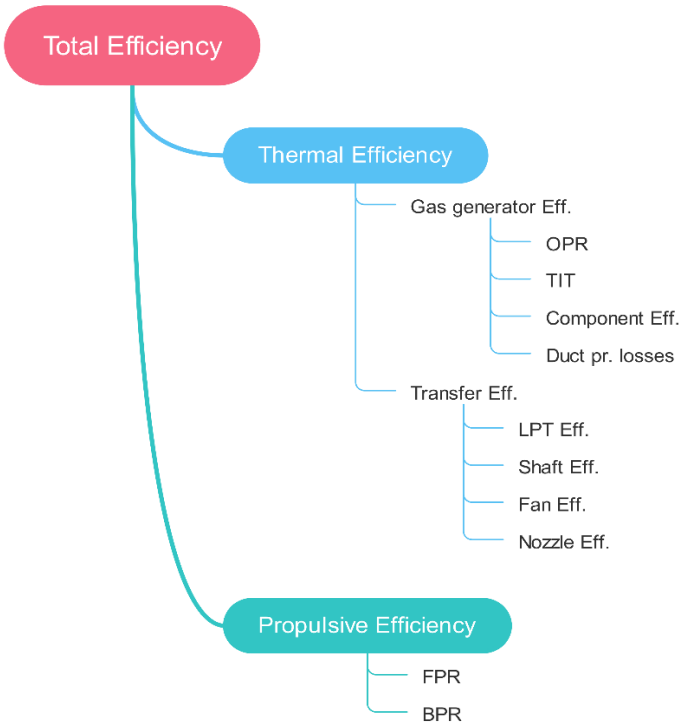


**Figure 13: Efficiency build-up of a gas turbine.**

$$\eta_{thermal} = \frac{P_{K.E\ jet}}{P_{chemical}+P_{electrical}} \quad (4)$$

$$\eta_{propulsive} = \frac{P_{thrust}}{P_{K.E.jet}} \quad (5)$$

Firstly, a sensitivity analysis is performed to LEAP-1A26's propulsive efficiency by varying BPR and FPR as shown in Fig. 14. A similar analysis was performed in reference [27]. The OPR, TIT and thrust are kept constant while varying the fan duct pressure ratio, BPR and air mass flow at the reference design point. It can be seen that for each FPR, there is a specific BPR at which the TSFC is minimum (due to the ideal jet velocity ratio [27]). The general trend is that lower fan duct PR's can achieve a lower TSFC at higher BPRs. Minimum TSFC is obtained at a fan duct PR of 1.48 with a BPR of 12.75. The TSFC is reduced by 1.3% but the mass flow rate through the fan is increased by 12%, compared to the LEAP-1A26 baseline model. When considering the drawbacks of increasing the engine diameter (larger fan, nacelle etc), it can be concluded that increasing the BPR further is not a viable option.


Copyright © 2020 by ASME

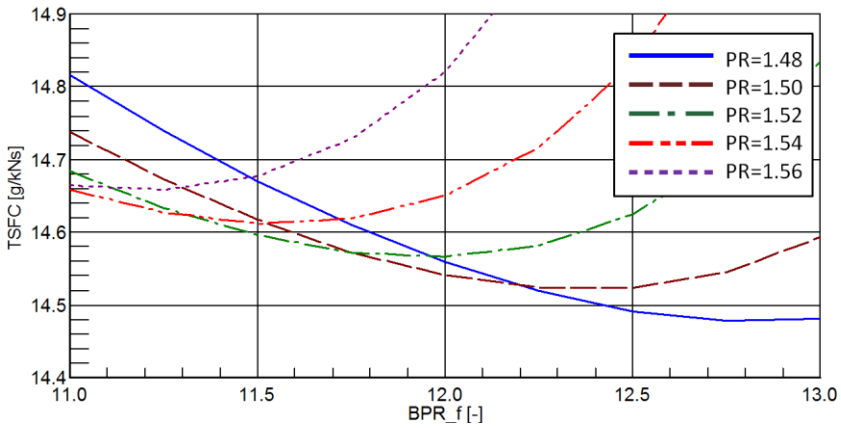


**Figure 14: Propulsive efficiency analysis of the baseline turbofan for various fan duct pressure ratios and BPRs at cruise thrust**

Figure 15 shows the OPR of the EATF at TOC. In the case of DDTF LEAP-1A26, the OPR can be increased by 2.3% with a power split of 14%, because it needs to operate at an LP-power fraction of 0.6 or below in order to meet the SM requirements. In case of a GTF, the transonic LPC is less limited by the surge margin, thereby allowing an increase of the OPR by 3.4%. In terms of the reduction in TIT during take-off, the DDTF and GTF show a similar reduction. For the case with 14% power split, the TIT is reduced by around 100 K for take-off as well as in TOC.

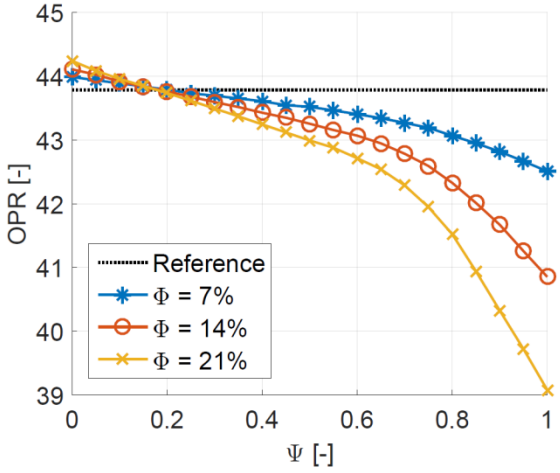


**Figure 15: OPR under different power splits and power fractions at TOC conditions**

Since a GTF with its different LPC performance map shows a larger potential for improvements with an EATF as compared to a DDTF, the GTF architecture is used for the rest of the results. Because the OPR and TIT change for the redesigned EATF, a new propulsive efficiency analysis need to be carried out to find the new optimum fan duct PR and BPR. Therefore, a similar analysis is carried out with the GTF as was shown in Fig. 14. In this case, the TIT increased from 1550 K to 1650 K while the increase of OPR is obtained by increasing the HPC PR from 14.5 to 15.0. The results show that the cruise TSFC can be reduced by 1.7% with a bypass fan PR of 1.50 and a BPR of 13.75. However, this would still require a relatively large increase in the air mass flow by 6.5%. If on the other hand the fan duct PR of 1.54 is selected with a BPR of 12.75, the TSFC is reduced by 1.0%, while the mass flow does not change (-0.01%). This second option is therefore selected and will be used in the rest of the analysis. It should be noted that the increased TIT will have a negative effect on the lifetime of the combustion chamber and HPT (since the materials will degrade faster). Since the focus of this study is on the performance aspects, the component life is not taken into account.

### 3.3. Mission Analysis

For the mission analysis, two technology levels have been used to assess the possible fuel savings and the feasibility of a HEPS. Table 3 shows the assumed technology levels for the years 2030 and 2040.

**Table 3: Different technology levels**

| Parameter: | 2030 | 2040 |
|---|---|---|
| Battery energy density | 600 Wh/kg | 1200 Wh/kg |
| Battery discharge efficiency: | 97.5% | 99% |
| EM power density: | 12.5 kW/kg | 25 kW/kg |
| EM maximum efficiency: | 97.5% | 99% |
| Inverter power density: | 20 kW/kg | 25 kW/kg |
| Inverter efficiency: | 99% | 99.5% |

Figure 16 compares the fuel consumption of the baseline A320neo, together with a HEP A320neo for the technology of 2030 (called $A320HEP_{2030}$) and the $A320HEP_{2040}$ which has the technology of 2040. The $A320HEP_{2030}$ shows a total fuel consumption reduction of 4.7%, whereas the $A320HEP_{2040}$ obtains a reduction of 7.3% with respect to the A320neo. Because of the assumed technological improvements in the year 2040, the weight penalty of the HEP on the aircraft would be smaller. The weight penalties are 5.5% and 2.5% for the


Copyright © 2020 by ASME

A320HEP$_{2030}$ and the A320HEP$_{2040}$, respectively. The most significant savings of both HEP aircraft are however expected during the taxi phases. For the A320HEP$_{2030}$, the more savings are obtained during the taxi phase than for the entire mission, indicating the HEPS is not able to save fuel during the cruise flight. With the A320HEP$_{2040}$, the marginal fuel savings can be realized during the cruise phase, wherease, the majority of fuel-saving is still obtained from electric taxiing.

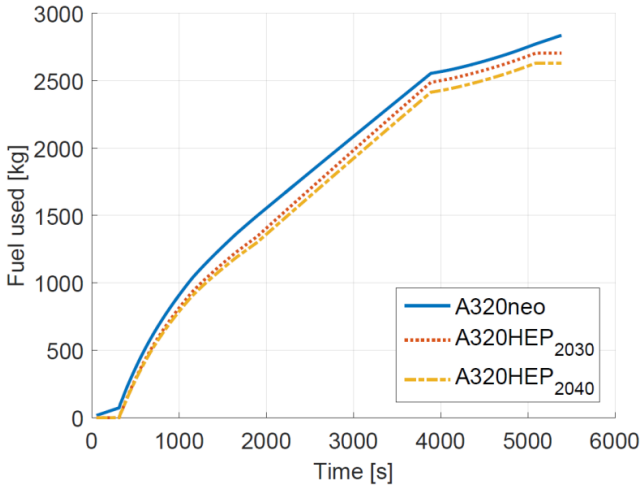


**Figure 16: Comparison of total fuel consumption between the A320neo and the A320HEP$_{2030}$ and A320HEP$_{2040}$ with redesigned EATF**

In the mission profile considered, the taxi-out and taxi-in were 5 minutes for each. The warmup or cooling-down time of the gas turbines was not taken into account. In reality, it is important to include the warm-up and cooling-down time for the safety and the longevity of the engine. Typically, the warm-up phase lasts for around 4 minutes, while 3 minutes is required for cooling down after touch down [28]. Because the turbofan needs to work at idle, enough thrust is available, and no additional electric power is required from the electric motors. A mission analysis, with warm-up and cooling down taken into account, shows that the savings of the A320HEP$_{2030}$ are reduced from 4.7% to 1.8%. Clearly, the taxi phase is determining the possible fuel savings. In 2007, the average US taxi time was significantly longer, at 17 minutes and 7 minutes for the taxi-out and taxi-in respectively [29]. Combining this longer taxi phase with the warm-up and cooling down would allow a fuel reduction of 7.1% with the A320HEP$_{2030}$ compared to the A320neo. Although these savings are significant, the lack of fuel-saving during the cruise flight means that EATF is not very promising. Therefore an electric taxiing system at the ground level is beneficial from an operational point of view.

## 4. CONCLUSIONS AND OUTLOOK

In this paper, a parallel hybrid electric turbofan has been investigated by means of a 0-D thermodynamic cycle modelling in GSP. The analysis was focussed on analysing the propulsion system performance, while the airframe, aircraft mission and MTOW were not altered. Several conclusions can be drawn from this research:

- The analysis shows that two electric motors, one on the LP-shaft and one on the HP-shaft, is required for achieving maximum efficiency while keeping a safe surge margin for LPC.
- A GTF architecture with a transonic LPC has a better potential for EATF than a DDTF due to better SM compared to a subsonic LPC.
- Due to the added electrical power, the TIT of the gas turbine decreases for a given thrust in take-off as well as climb phase.
- However, for the cruise condition, the OPR and TIT of a redesigned EATF can be increased. By applying a power split ratio of 14% for both take-off and climb phases, the redesigned turbofan with higher OPR and TIT shows a cruise TSFC reduction of 1.0%.
- The potential block fuel savings for a parallel HEP version of the existing A320 aircraft are limited, mainly due to the additional mass of the required electrical system. The total weight of the aircraft increases by around 5.5% with expected technology for the year 2030, and 2.5% for 2040 technology level.
- The study shows that this additional weight cannot sufficiently be offset by the 1.0% reduction in the cruise thrust specific fuel consumption.
- Over a typical mission of 1000 km, a fuel saving of 4.7% can be achieved with an anticipated technology level of 2030. The fuel reduction can be increased to 7.3% with the anticipated technology levels of 2040.
- With the anticipated 2030 technology level, the main fuel savings are achieved during the taxi phase, whereas the other flight phases do not show a substantial reduction in fuel consumption.
- Therefore fuel savings can be better realised by using ground-based electric taxiing instead of a complete hybrid-electric propulsion system.
- For 2040 technology level, some fuel savings are also achieved during the cruise flight. However, the majority of fuel-saving is still achieved from electric taxiing.
- Taking into account the warm-up and cooling down requirements of a turbofan engine and applying more realistic taxi phase lengths (17 and 7 minutes for taxi-out and taxi-in respectively), the expected fuel savings are around 7.1% for the A320 with a HEPS.
- Despite the fuel savings and benefits of electric taxiing with a HEPS, commercial parallel HEP aircraft are not expected to be introduced in the coming two decades. HEPS will require a significant redesign of the aircraft propulsion system, while the majority of the fuel savings can be achieved by incorporating an electric taxiing system as a ground-based electric taxi system will require less effort to be developed than a HEPS.


Copyright © 2020 by ASME

REFERENCES


[1] European Commission, "Flightpath 2050: Europes Vision for Aviation.," Luxembourg, Luxembourg, 2011.

[2] A. Klauber and I. Toussie, "A Radical New Plan for Aviation," in *In World Economic Forum*, Davos, Switzerland, 2019.

[3] D. Lee, D. Fahey, P. Forster, P. Newton, R. Wit, L. Lim, B. Owen and R. Sausen, "Aviation and global climate change in the 21st century," *Atmospheric Environment,* vol. 43, nr. 22-23, pp. 3520-3537, 2009.

[4] J. Gladin, C. Perullo, J. Tai and D. Mavris, "A Parametric Study of Hybrid Electric Gas Turbine Propulsion as a Function of Aircraft Size Class and Technology Level," in *55th AIAA Aerospace Sciences Meeting*, Grapevine, Texas, 2017.

[5] A. Ang, A. Gangoli Rao, T. Kanakis and W. Lammen, "Performance analysis of an electrically assisted propulsion system for a short-range civil aircraft," *Proceedings of the Institution of Mechanical Engineers, Part G: Journal of Aerospace Engineering,* vol. 233, nr. 4, pp. 1490-1502, 2019.

[6] M. Bradley and C. Droney, "Subsonic Ultra Green Aircraft Research: Phase II Volume II Hybrid Electric Design Exploration," NASA/CR–2015-218704, 2015.

[7] M. Hoogreef, R. Vos, R. de Vries and L. Veldhuis, "Conceptual Assessment of Hybrid Electric Aircraft with Distributed Propulsion and Boosted Turbofans," in *AIAA Scitech Forum*, San Diego, California, 2019.

[8] A. Seitz, M. Nickl, A. Stroh and P. Vratny, "Conceptual study of a mechanically integrated parallel hybrid electric turbofan," *Proceedings of the Institution of Mechanical Engineers, Part G: Journal of Aerospace Engineering,* vol. 232, nr. 14, pp. 2688-2712, 2018.

[9] V. Kloos, T. Speak, R. Sellick and P. Jeschke, "Dual Drive Booster for a Two-Spool Turbofan: High Shaft Power Offtake Capability for More Electric Aircraft and Hybrid Aircraft Concepts," *Journal of Engineering for Gas Turbines and Power,* vol. 140, nr. 12, p. 121201, 2018.

[10] Japan Aircraft Development Corporation, "Worldwide Market Forecast 2018 – 2037," Tokio, Japan, 2018.

[11] GSP Development Team, "GSP manual," 2015.

[12] The MathWorks Inc, "Matlab R2015b (8.6.0)," 2015.

[13] P. Walsh and P. Fletcher, Gas Turbine Performance, 2nd red., Oxford, United Kingdom: Blackwell, 2004.

[14] W. Visser, "Generic Analysis Methods for Gas Turbine Engine Performance," PhD Thesis, TU Delft, 2015.

[15] ICAO, "LEAP-1A26," in *ICAO ENGINE EXHAUST EMISSIONS DATA BANK*, 2019.

[16] Airbus, "Airbus A320 Aircraft Characteristics and Maintenance Planning," Blagnac, France, 2018.

[17] Lissys Limited, *PianoX,* 2010.

[18] N. Cumpsty, "Preparing for the Future: Reducing Gas Turbine Environmental Impact—IGTI Scholar Lecture," *Journal of Turbomachinery,* vol. 132, nr. 4, p. 041017, 2010.

[19] IHS Markit, "CFM International CFM56," in *Jane's Aero-Engines*, 2018.

[20] IHS Markit, "Airbus A320," in *Jane's All the World's Aircraft*, 2017.

[21] CFM International, *CFM LEAP Brochure,* 2010.

[22] EMRAX, "Technical Data and Manual for EMRAX Motors/Generators," 2018.

[23] D. Moreels and P. Leijnen, "High-Efficiency Axial Flux Machines", *White Paper Magnax Axial Flux Machines V1.9,* 2018.

[24] J. Larminie and J. Lowry, "Electric Vehicle Technology Explained", 2nd red., Oxford, United Kingdom: John Wiley & Sons, Ltd., 2012.

[25] J. Pyrhönen, T. Jokinen and V. Hrabovcová, "Design of Rotating Electrical Machines," West Sussex, United Kingdom: John Wiley & Sons, Ltd, 2008.

[26] R. McDonald, "Electric Propulsion Modeling for Conceptual Aircraft Design," in *52nd Aerospace Sciences Meeting*, National Harbor, Maryland, 2014.

[27] K. Kurzke and I. Halliwell, "Propulsion and Power: An Exploration of Gas Turbine Performance Modeling," Cham, Switzerland: Springer International Publishing, 2018.

[28] Y. Nicolas, "eTaxi, taxiing aircraft with engines stopped," *Airbus Technical Magazine - Fast 51,* pp. 2-10, January 2013.

[29] B. Goldberg and D. Chesser, "Sitting on the Runway: Current Aircraft Taxi Times Now Exceed Pre-9/11 Experience," U.S. Department of Transportation, 2008.



Copyright © 2020 by ASME